Published in final edited form as:
Soft Matter. 2013 February 28; 8(8): 2423–2431. doi:10.1039/C2SM06969E.

Antibacterial Biomimetic Hybrid Films

M. Carme Coll Ferrer[†,±], **Noreen J. Hickok**[§], **David M. Eckmann**[‡,*], and **Russell J. Composto**[±,*]

M. Carme Coll Ferrer: macoll@seas.upenn.edu; Noreen J. Hickok: Noreen.Hickok@jefferson.edu; David M. Eckmann: David.Eckmann@uphs.upenn.edu; Russell J. Composto: composto@seas.upenn.edu

[†]The Institute for Medicine and Engineering, University of Pennsylvania, Philadelphia, PA 19104, US

[‡]Department of Anesthesiology and Critical Care, University of Pennsylvania, Philadelphia, PA 19104, US

[±]Department of Materials Science and Engineering, University of Pennsylvania, Philadelphia, PA 19104, US

[§]Department of Orthopaedic Surgery, Thomas Jefferson University, Philadelphia, PA 19107, US

Abstract

In this work, we present a novel method to prepare a hybrid coating based on dextran grafted to a substrate and embedded with silver nanoparticles (Ag NPs). First, the Ag NPs are synthesized *in situ* in the presence of oxidized dextran in solution. Second, the oxidized dextran is exposed to an amine functionalized surface resulting in the simultaneous grafting of dextran and the trapping of Ag NPs within the layer. The NP loading is controlled by the concentration of silver nitrate, which is 2 mM (DEX-Ag2) and 5 mM (DEX-Ag5). The dried film thickness increases with silver nitrate concentration from 2 nm for dextran to 7 nm and 12 nm for DEX-Ag2 and DEX-Ag5, respectively. The grafted dextran film displays features with a diameter and height of ~ 50 nm and 2 nm, respectively. For the DEX-Ag2 and DEX-Ag5, the dextran features as well as individual Ag NPs (~ 5 nm) and aggregates of Ag NPs are observed. Larger and more irregular aggregates are observed for DEX-Ag5. Overall, the Ag NPs are embedded in the dextran film as suggested by AFM and UVO studies. In terms of its antimicrobial activity, DEX-Ag2 resists bacterial adhesion to a greater extent than DEX-Ag5, which in turn is better than dextran and silicon. Because these antibacterial hybrid coatings can be grafted to a variety of surfaces, many biomedical applications can be envisioned, ranging from coating implants to catheters.

Keywords

Antibacterial coatings; Dextran; Silver Nanoparticles; Hybrid film; S. aureus

1. Introduction

The next generation of novel biomaterials should be both biocompatible and antibacterial. Presently, biomaterial interactions with blood, including thrombus formation and possible colonization by bacteria, necessitate post-operative prophylactic therapies. Examples include recently FDA-approved implant devices such as the left ventricular assist system (HeartMate II) and the implantable heart (AbioCor®) in which the patient is required to take anticoagulant medications to prevent clotting-related complications[1, 2]. Thus, in a strict

[*]Russell J. Composto Phone: (215)-898-4451; Fax: (215)-573-2128; composto@seas.upenn.edu; David M. Eckmann Phone: (215)-349-5348; Fax: (215)-349-5078; David.Eckmann@uphs.upenn.edu.

sense, these devices are not truly biocompatible. Moreover, as these devices have no antimicrobial activity, should infection establish, the devices must be surgically explanted.

To develop advanced multifunctional biocompatible biomaterials we aim to mimic the endothelial glycocalyx, a polysaccharide-rich layer that protects the endothelium and plays a critical role in controlling blood flow, ion and water transport as well as molecular adhesion.[3] Among natural polysaccharides, dextran has shown outstanding properties against nonspecific protein adhesion.[4–8] Piehler *et al.* studied protein interactions in dextran layers covalently attached by silane chemistry onto silicon wafers.[6] They observed shielding of non-specific proteins with thick dextranized surfaces (up to 8 ng/mm^2). Ombelli *et al.*, employing similar silane chemistry, demonstrated that dextranized surfaces strongly suppress fibrinogen and bovine serum albumin relative to bare silicon and 3-aminopropyltriethoxysilane-activated silicon surfaces.[7] In addition, dextran-coated surfaces, prepared on polyethylene terephthalate and glass, reduced cell adhesion and proliferation as demonstrated by Massia *et al.*[9]

To enhance the antibacterial properties of a biomaterial, we propose to incorporate silver nanoparticles (Ag NPs) into dextran. Ag NPs, are well-known antibacterial agents, whose antimicrobial properties stem from their oxidation to the +1 ionization state.[10] At low concentrations (0.5 μg/mL), silver has been shown to have high efficacy against Gram positive and Gram negative bacteria and fungi.[11] Even though the mechanism is not well understood, it has been demonstrated that silver can disrupt a broad range of biological processes in microorganisms. For instance, silver binds to thiols or disulfide groups in cell wall proteins causing ion leakage and cell rupture.[12] Inside the cell, silver binds and denatures DNA and RNA, thereby inhibiting replication.[13] Because of their antimicrobial properties, Ag NPs are receiving widespread attention in medical applications. Products containing Ag NPs are found in several over-the-counter products, such as Curad® silver bandages. Additionally, Ag NPs have potential use as surface coatings for medical instruments,[14] catheters[15] and water purification systems.[16]

Polysaccharides have been employed to synthesize and stabilize silver nanoparticles in solution as well as to prepare coatings and polymer-silver nanocomposites.[17–21] In solution, heparin, a negatively charged polysaccharide, has been used to prepare Ag NPs,[20] whereas Huang *et al.* utilized autoclaving to synthesize and stabilize Ag NPs inside the helical amylase chain of starch.[17] Travan *et al.* reported the formation of Ag NPs using a derivative of chitosan with and without ascorbic acid as a reducing agent.[22] The former was evaluated against bacteria in solution as was a 3D gel structure prepared by mixtures containing alginate; both were found to be very effective toward Gram positive and Gram negative bacteria while not showing any cytotoxic effect towards cells. This chitosan derivative was also used to coat a methacrylic thermoset via electrostatic interactions while maintaining the inherent antimicrobial and non-cytotoxic properties of the solution. However, the resulting coating was thick, approximately 10–15 μm, and rough with clusters of silver of up to 1 μm in size. In addition, Ag NPs have been incorporated in semi interpenetrating hydrogel networks of poly(acrylamide) and dextran[23] or other carbohydrates, i.e., gum acacia, carboxymethylcellulose and starch.[21] The reduction of Ag NPs in these hydrogel networks required alkaline solution for dextran-based hydrogel or a reducing agent, i.e., sodium borohydride for the other polysaccharide-based hydrogels. These hydrogel-Ag nanocomposites showed improved antibacterial efficiency against Gram positive bacteria compared to the pure hydrogels.

In this work, we explore the feasibility of producing thin hybrid coatings (~ nm) synthesized following a unique route. These thin films are directed towards two major clinical applications, the prevention of vascular catheter related bloodstream infection (CRBSI) and

ventilator-associated pneumonia (VAP). Both CRBSI and VAP are associated with high patient morbidity, mortality, increased length of hospital stay, and accompanying health care costs of $2 billion and $10 billion per year, respectively, for infections involving multiple pathogens.[24–28] CRBSIs are among the most common nosocomial infections in intensive care unit (ICU) patients and are estimated to occur in 3 to 7% of catheters used. As many as 250,000 patients are affected annually in the United States,[29] with 20,000 central venous catheter related infections occurring each year. VAP occurs in 9% to 18% of mechanically ventilated patients within 10 days after endotracheal intubation. Both VAP and CRBSI result when microorganisms adhere to the biomaterial surface of the vascular catheter or endotracheal tube, which establishes favorable in vivo conditions for bacterial proliferation and biofilm formation. A combination of reduced metabolism, cross-talk and changes in gene expression alter the availability of bacterial targets of antibiotic action.[30] The biofilm itself can filter out antibiotics or secrete factors that reduce antibiotic concentration within the biofilm. These mechanisms contribute to antibiotic resistance within the biofilm,[31, 32] rendering conventional oral, topical or intravenous antibacterial treatments inadequate. Thus, more complex, permanent thin film surface coatings are sought to inhibit CRBSIs and VAP over the course of days to weeks, consistent with clinical use of vascular catheters and endotracheal tubes. Useful surface coatings will minimize or eliminate bacterial growth, thus subverting the progression from adherent bacterium to biofilm-encased colonies populating the biomaterial surface to eventual dissemination of bacterial colonies into the bloodstream or deep into the lung.

With this in mind, we develop a method to covalently attach dextran to surfaces in the presence of Ag NPs, which remain entrapped in the dextran layer. First, Ag NPs are synthesized *in situ* in a dextran solution, which is subsequently grafted to the surface. The loading of Ag NPs entrapped in the grafted dextran is studied as a function of the initial concentration of silver ions. Two concentrations of silver nitrate are studied, 2 mM and 5 mM, referred to herein as DEX-Ag2 and DEX-Ag5, respectively. The attachment of dextran embedded with Ag NPs on silicon is carried out via silane chemistry. The grafted coatings are characterized by UV-VIS spectroscopy, atomic force microscopy (AFM) and Rutherford backscattering spectrometry (RBS). A uniform distribution of Ag NPs embedded within the film is observed. The Ag NPs are 5 nm in diameter as measured by TEM and AFM with the presence of aggregates. Larger aggregates are observed for the DEX-Ag5 films. The antibacterial activity of the coatings is tested against *Staphylococcus aureus* (*S. aureus*). The hybrid films show reduction in bacteria colonization when compared to control surfaces. Relative to silicon and bare dextran, DEX-Ag2 strongly reduces bacteria adhesion by 93% and 78%, respectively.

2 Experimental section

2.1 Materials and instruments

All solvents and reagents were of analytical grade and used as received. Dextran from Leuconostoc *ssp.* (Mw = 100 kDa) was purchased from Fluka Chemie. 3-aminopropyltriethoxysilane (APTES), sodium periodate ($NaIO_4$), sodium cyanoborohydryde ($NaBH_3CN$) and silver nitrate ($AgNO_3$) were purchased from Sigma-Aldrich Co. Silicon wafers (CZ silicon; type, N; dopant, Ph) were acquired from SiliconQuest Int'l. *S. aureus* (ATCC™ 35556®) was obtained from PML Microbiologicals. Brain heart infusion (BHI), BBL™ trypticase™ soy broth (TSB), Bacto™ agar, and phosphate buffered saline tablets (PBS) were purchased from Fisher Scientific. All solutions for bacterial test were sterilized by autoclaving.

The film thickness was measured using an Auto-El-II Null ellipsometer (Rudolph Research, Flanders, NJ) at a fixed incident angle of 70° with a helium-neon laser source (λ = 6328 Å).

All measurements were collected within 1–2 h of sample preparation to minimize contamination. The thickness of the aminated and the polysaccharide layer were determined using a fixed refractive index of 1.462. Water contact angles were measured using a 1 μL sessile drop at ambient conditions. Images were captured via a CCD camera. The contact angle at the three phase boundary was measured with ImageJ (NIST). UV spectra of silver nanoparticles in oxidized dextran solution as well as grafted dextran containing silver nanoparticles on glass were recorded on a Varian spectrophotometer (Cary 5000 UV-vis-NIR). The modified glass surfaces were prepared following the same method as for silicon wafers. Surface topography images were recorded using atomic force microscopy (AFM, Pico Plus, Agilent Technologies, Santa Clara, CA). Images were obtained using TOP MAC tapping mode with Type II Mac levers (Agilent Technologies). Images were analyzed using Gwyddion (Czech Metrology Institute). The amount of silver in the grafted dextran was determined by Rutherford backscattering technique (RBS), using $4He^{++}$ ions accelerated to 2 MeV, with the beam at normal incidence to the sample and a backscattering angle of −5°. Experimental RBS curves were fitted with those obtained by numerical simulation using RUMP software (Computer Graphics Service). The chemical composition of the layer and the corresponding number of silver atoms/cm were used as fitting parameters. The silver nanoparticles were investigated by transmission electron microscopy (TEM) on a JEOL JEM 2010 at 80 kV. The samples were prepared by placing a dilute drop of the nanogel solution onto a holey carbon TEM grid (Structure Probe, Inc.). The excess of liquid was removed by capillary reaction using a paper filter below the TEM grid. TEM micrographs were analyzed using ImageJ (NIST). The average diameter (± standard deviation) of the silver nanoparticles was obtained by measuring 330 nanoparticles.

2.2 Oxidation of dextran

$NaIO_4$ was added to 20 mL of an aqueous solution of dextran (50 mg/mL) in a 1:1 molar ratio. The solution was vigorously stirred in the dark at room temperature until a clear yellow solution was obtained (6h). The resulting oxidized dextran was purified from iodate (IO_3^-) and unreacted periodate (IO_4^-) by extensive dialysis against water using a semi-permeable, regenerated cellulose dialysis tubing (MW cutoff 15 kDa, Spectrum Labs) for at least 3 days. The purified oxidized dextran solution was then lyophilized. The percentage of oxidation was determined by the hydroxyl amine hydrochloride colorimetric titration method.[33] Briefly, oxidized dextran is reacted with hydroxyl amine hydrochloride in methylene orange to produce a dextran polyoxime while releasing a hydrochloric acid equivalent for each formyl residue. The hydrochloric acid released is then quantified by colorimetric titration using sodium hydroxide. After oxidation, dextran is purified from iodated and unreacted periodate by extensive dialysis and lyophilized.

2.3 Synthesis of silver nanoparticles

An aqueous solution of $AgNO_3$ (2 mM or 5 mM) was added to 2 mL of an aqueous solution of oxidized dextran (1 g/L). The mixture was placed on an oil bath and heated at 70 °C for 55 minutes, with magnetic stirring.

2.4 Amination of the substrates

Silicon wafers were cleaned by immersion in “piranha” solution (70% H_2SO_4 and 30% H_2O_2) for 20 min at 80 °C, washed with copious amounts of water, and then soaked in water until used. Prior to use, the surfaces were blown dry with compressed N_2 (g) and exposed to UVO (ultraviolet-ozone) light in a UVO-cleaner (UVO Cleaner model 42, Jelight Co. Inc.) for 10 min to form a uniform oxide layer (1.6 ± 0.2 nm). Subsequently, surface amination was carried out using the vapor deposition method. Specifically, samples were placed face up on the bottom of a glass jar (500 mL) with an open vial containing 1 mL APTES, the jar was sealed and the reaction was allowed to proceed for 3 h at 70 °C.

2.5 Grafting of Ag NPs-dextran onto aminated surfaces

10 mg of $NaBH_3CN$ were added to 3 mL of a freshly made aqueous solution of silver nanoparticles in oxidized dextran. The solution was hand shaken and poured onto Petri dishes containing the freshly APTES-modified silicon wafers substrates. The Petri dishes were left in dark conditions overnight on an orbital shaker. After dextran immobilization, the wafers were removed from solution, rinsed with deionized water (5 x 1 mL) and blown dry with compressed N_2 (g).

2.6 Bacterial culture and antibacterial testing

Sterilized silicon oxide, dextran and dextran embedded with Ag NPs surfaces were tested for bacterial adhesion following the method described by Lee *et al.*[34] *S. aureus* (ATCC 35556) was cultured in BHI broth at 175 rpm and 37 °C during 12–16 h (overnight culture) and diluted to ~ 10^4 cfu/ml using a 0.5 McFarland standard, a turbidity standard equivalent to 10^8 cfu/ml. The surfaces were incubated in the diluted bacterial solutions at 100 rpm and 37 °C for 6 h. Non-adherent bacteria were rinsed off by incubating the samples in PBS at 100 rpm and 37 °C for 20 min. Rinsed samples were air dried (2 min), and incubated under a thin film of TSB agar (3 wt%) at 37 °C for 12–16 h (overnight) to allow any adherent bacteria to grow into colonies. Surface colonization was imaged by optical microscopy. The numbers of colonies were counted using ImageJ and the colony counts were normalized to an area of 1 x 4/3 cm. All experiments were performed at least three times and for each surface type, a minimum of four images was used to determine average (± standard deviation) colony counts per unit area.

3. Results

3.1 Oxidation of dextran

Dextran is oxidized with sodium periodate under mild conditions, i.e., room temperature, 1:1 molar ratio. The reaction pathway involves the rupture of anhydroglucose units to form formyl groups, as illustrated in Figure 1. Following this method, oxidized dextrans with 5% aldehyde content are obtained as determined by the hydroxyl amine hydrochloride colorimetric titration method.[33]

3.2 *"In situ"* synthesis of silver nanoparticles

The formation of Ag NPs is indicated by a change of the colorless DEX solution to yellow. The colloidal Ag is stable in DEX-Ag2 (i.e., bright yellow solution in Figure 1) for at least 8 h. However, the Ag NPs are less stable in the DEX-Ag5 solution and larger aggregates are formed within 1 h as indicated by a change in the solution color (i.e., solution turns orange) as shown in Figure 2. The formation of Ag NPs in DEX solution is also confirmed by UV-VIS spectroscopy. UV-VIS spectra of DEX-Ag2 and DEX-Ag5 in solution are shown in Figure 3a. A strong resonance due to the silver surface plasmon vibration is observed at 412 nm for both DEX-Ag solutions. Additionally, the breadth of the UV-VIS spectra reflects the dispersion/aggregation of NPs, which in our studies depends on the initial $AgNO_3$ concentration. The Ag NPs in DEX-Ag2 are well dispersed as shown by one main narrow peak having a peak width at half maximum (PWHM) = 89 nm. For DEX-Ag5 a peak associated with small individual particles is observed near 412 nm. However, a broad shoulder is now observed as noted by the increase in the PWHM to 197 nm. Note that this shoulder is also observed for DEX-Ag2 although its intensity is much smaller.

Furthermore, Ag NPs embedded in DEX-Ag2 are investigated by TEM. A representative TEM micrograph is shown in Figure 3. The Ag NPs are spherical with an average of 4.8 ± 2.7 nm in diameter. These results are in agreement with previous studies reported in the literature. Vinod *et al.* using a natural hydrocolloid solution (gum kondagogu) to stabilize

Ag NPs observed, Ag NPs of 5.5 ± 2.5 nm in diameter by TEM at the same UV wavelength.[35]

3.3 Covalent attachment of dextran to surfaces and simultaneous embedding of Ag NPs

Prior to attaching the dextran containing Ag NPs to silicon, the wafers are activated by vapor deposition of amine-terminated silane molecules, 3-aminopropyltriethoxy silane (APTES). The resulting aminated surfaces are 1 ± 0.3 nm thick. Subsequently, the dextran solution containing Ag NPs is grafted to the amine-derived substrates by immersing them into the colloidal solution in the presence of a reducing agent, sodium cyanoborohydride ($NaCNBH_3$). The mechanism is illustrated in Figure 4. The aldehydes from oxidized dextran react with the amines from the surface to form imines, which are reduced to amines with sodium cyanoborohydride. Film thickness and contact angle of the grafted dextranized surfaces and dextranized surfaces containing silver nanoparticles are reported in Table 1. The film thickness increases with the presence of Ag NPs. While purely oxidized dextran films are thinner than 2 nm (i.e., 1.6 ± 0.2 nm), thicknesses of around 7 nm (i.e., 6.7 ± 0.5 nm) and 12 nm (i.e., 12 ± 5 nm) are obtained for DEX-Ag2 and DEX-Ag5, respectively. In contrast, the contact angle of water on the hydrophilic dextran is ~ 20°, which is similar to the values for DEX-Ag 2 and DEX-Ag5. Because water wets silver, this result indicates that the Ag NPs are mostly embedded within the dextran coating.

The presence of Ag NPs in the dextran grafted surfaces is further confirmed by UV-VIS spectroscopy. The UV spectra of films prepared from DEX-Ag2 and DEX-Ag5 solution are shown in Figure 3b. The silver surface plasmon resonance of the modified surfaces appears at 400 nm which is slightly lower than 412 nm observed in solution. This shift in wavelength is related to the change in the local refractive index of the medium. As previously reported,[36] the surface plasmon resonance of silver nanoparticles is highly sensitive to small changes in refractive index, and undergoes a blue shift as the local index decreases in agreement with our studies (Figure 3). As the refractive index (n_D) decreases from water (n_D = 1.34) to air (n_D = 1), the surface plasmon resonance of the Ag NPs experiences a blue shift (412 vs 400 nm). Regarding the breadth of the spectra, the spectrum for DEX-Ag2 shows a Gaussian-like peak, which is an indication of uniform and dispersed Ag NPs, whereas the spectrum for DEX-Ag5 shows a broader peak with a long tail extending towards higher wavelength indicating the presence of aggregates of Ag NPs.

3.4 Surface characterization of hybrid films

The surface morphology, roughness and average feature height (AFH) are studied using tapping mode AFM. Representative topography images over 2 x 2 μm^2 scan areas of dextran and silver embedded dextran surfaces with their corresponding line scan (white line) are shown in Figure 5. In agreement with previous studies,[37] topographic images of dextranized surfaces display patches with a diameter of ~ 50 nm and a height of 2 nm. As noted in images compared at similar z-scales, this characteristic morphology is not disrupted by the presence of Ag NPs, which are integrated into the film. The line scans for DEX-Ag2 and DEX-Ag5 were chosen in areas free of large aggregates to confirm that the inherent texture of the DEX surface is retained. Whereas the DEX-Ag2 film exhibits a uniform dispersion of small Ag NPs and moderate sized aggregates, larger irregular aggregates are present in the DEX-Ag5. The presence of Ag NPs and larger aggregates is also reflected in the surface roughness, R_{rms} and AFH values, summarized in Table 1. The surface roughness values for DEX-Ag surfaces are larger than for the DEX surface, namely R_{rms} is 0.5 ± 0.1 nm versus 4.2 ± 0.7 and 8.4 ± 2.3 nm for DEX-Ag2 and DEX-Ag5, respectively. The AFH results further support these results, as the values increase with increasing Ag concentration.

3.5 Characterization of Ag NPs after dextran removal

To further investigate the silver embedded in the dextran film, the surfaces were characterized by a combination of AFM and UVO techniques. Because UVO exposure removes dextran, the Ag NPs can be imaged by AFM. Topographic images of DEX-Ag2 surfaces before and after UVO exposure and their corresponding phase images are shown in Figure 6. Before UVO exposure, the surfaces show a uniform distribution of Ag NPs and few aggregates. However, after 15 min UVO exposure, the dextran is removed and a larger number of Ag NPs are observed, confirming that some of the Ag NPs below the surface are not observed in the DEX-Ag2 film. Furthermore, the post-UVO treated films were examined by UV-VIS spectroscopy (data not shown). As expected the peak broadened with UVO time due to Ag NPs aggregation as shown by AFM images in Figure 6.

3.6 Silver loading and stability in DEX-Ag2 and DEX-Ag5 films

The weight percentage (wt%), of silver in the hybrid coatings is analyzed using RBS. Figure 7 shows the RBS spectra for DEX-Ag2 and DEX-Ag5. Backscattering from silver atoms near the surface appears at channel 270. The silver wt% is determined by fitting a theoretical model to the experimental data. Initially, both DEX-Ag2 and DEX-Ag5 contain about 7–8 wt% of Ag. Even though both films have similar Ag content, RBS spectra indicate some differences in the Ag distribution. For DEX-Ag2, the Ag is uniformly dispersed as noted by the sharp edges and flat top of the yield. Although the Ag is also uniform in the DEX-Ag5 film, the large aggregates result in a rougher surface that broadens the back edge of the yield. These results further support UV-VIS and AFM studies. RBS was also used to measure stability of silver in DEX-Ag2 and DEX-Ag5. Samples were incubated using similar conditions as the bacterial testing. After incubating the samples for 6 h at 37 °C and shaking at 100 rpm, RBS spectra were taken and shown as the red data in Figure 7. The reduction in the yield of Ag represents a 26 wt% and 18 wt% loss of Ag for the DEX-Ag2 and DEX-Ag5 films, respectively.

3.7 Bacteria Adhesion

Dextran films and silicon as a control as well as dextran films containing Ag NPs were incubated with *S. aureus* to measure bacterial adhesion. Control surfaces are more abundantly colonized than the dextran films which contain Ag NPs (Figure 8). Relative to silicon and dextran, DEX-Ag2 inhibits bacterial colonization by 93% and 76%, respectively. Although less effective, DEX-Ag5 also inhibits bacterial colonization. In particular, DEX-Ag5 reduces bacterial colonization by 86% and 54% relative to silicon and dextran, respectively. On the surfaces, marked differences in bacterial colony size are noted, with the largest colonies observed on DEX-Ag. This variation in colony size appears to correlate inversely with numbers of colonies, suggesting that nutrient deprivation in this static system may be the cause of the variability.

4. Discussion

In the field of biomaterials, polysaccharides are widely studied due to their biocompatibility and availability.[4–9, 38] Thus far, polysaccharides have been employed to synthesize and stabilize Ag NPs in solution.[17, 20, 39] For example, heparin a negatively charged polysaccharide, and starch, a neutral polysaccharide have been used. However, the latter required harsh conditions, i.e., autoclaving, to prepare stable colloidal silver.[17] Ag NPs have also been synthesized using starch under milder conditions but requires a stabilizing agent, i.e., glucose, and mild alkaline conditions.[39] Moreover, derivatives of polysaccharides, such as chitosan, have also been employed to synthesize Ag NPs with[19] and without[22] the addition of a reducing agent.

In this work, we focus for the first time on dextran, a neutral and biocompatible polysaccharide, to synthesize Ag NPs by the "*in situ*" reduction of $AgNO_3$. With this methodology, no other reducing or stabilizing agents are required other than dextran. In our approach, dextran is oxidized via periodate oxidation as illustrated in Figure 1. The rationale behind the use of mildly oxidized dextran for the "*in situ*" synthesis of Ag NPs is two-fold: (1) the hydrophilic hydroxides in DEX absorb the silver ions in solution, and (2) the aldehyde groups from DEX act as both a reducing and stabilizing agent of the nanoparticles. The reduction of the silver ions during the "*in situ*" formation of Ag NPs in DEX is evident by the change of the colorless solution to bright yellow. The initial concentration of this precursor, $AgNO_3$, is evaluated, in particular at 2 mM and 5 mM concentration (denoted as DEX-Ag2 and DEX-Ag5, respectively). Furthermore, the UV-VIS spectra (Figure 3) clearly show the presence of the surface plasmon resonance peak corresponding to silver near 412 nm. The breadth of the surface plasmon resonance reflects the dispersion of Ag NPs and indicates the presence of Ag NPs as well as larger aggregates in DEX-Ag5. Increasing the concentration of Ag^+ surpasses the stabilizing capabilities in DEX, leading to a colloidal silver solution that tends to aggregate over time. Evidence for aggregation includes a broadening of the peak as well as a change in color from yellow to orange (Figure 2).

The strategy for covalent attachment of dextran to a surface previously reported by our group[37] and by others[5, 9] has been adapted for this work and is illustrated in Figure 4. This methodology is based on aqueous conditions using low toxicity reagents and mild reaction conditions. Following "*in situ*" synthesis of Ag NPs, DEX embedded with Ag NPs is coupled by reductive amination to a previously aminated silicon wafer. Silane chemistry is used to functionalize the silicon wafer to form an aminated monolayer.

The presence of Ag NPs embedded in the DEX-Ag coatings is demonstrated by a combination of techniques, in particular ellipsometry and contact angle (Table 1), UV-VIS (Figure 3), AFM (Figure 5 and 6) and RBS (Figure 7). The loading of Ag^+ in the film results in an increase in film thickness while contact angle remains unaltered. The latter indicates Ag NPs are not located on the surface of the film but embedded within the film. The hybrid coatings show better dispersion of Ag NP at lower Ag^+ loading concentration, with an average diameter of 5 nm as indicated by UV-VIS, TEM and AFM. In contrast, higher Ag^+ loading for the DEX-Ag5 films, leads to 5 nm Ag NPs as well as larger aggregates. Overall, the amount of silver in the film remains relatively fixed and independent of the initial precursor loading, around 7–8 wt% as measured by RBS. The RBS also confirm that the Ag is uniformly distributed within the film rather than segregated to the surface.

The antibacterial efficiency of these hybrid coatings is demonstrated against a Gram positive bacterium, *S. aureus*. This pathogen is among the most commonly reported pathogens that cause deep infection in hospitals.[29] *S. aureus* is commonly carried on the skin or in the nose of healthy people and readily adheres to host proteins (e.g., fibrinogen, fibronectin) commonly adsorbed to biomaterials. This adherence can easily lead to formation of a biofilm that shelters and protects the pathogens against antimicrobial agents. Therefore, in order to combat contamination by *S. aureus* and other types of bacteria, it is vital to develop surfaces that resist or prevent bacterial colonization and subsequent biofilm formation. As a first test of antimicrobial efficacy, our surfaces were tested against bacteria in solution at 37 °C. Both hybrid coatings show reduced bacterial colonization compared to the control, dextran and silicon surfaces. In particular, DEX-Ag2 inhibits bacterial adhesion relative to silicon and dextran by 93% and 78% compared to 86% and 54% for DEX-Ag5, respectively. The slightly lower efficiency against bacterial adhesion of DEX-Ag5 is attributed to the presence of larger Ag aggregates compared to the better dispersed Ag NPs in DEX-Ag2. Even though both hybrid coatings have similar Ag content, as demonstrated by RBS, the presence of smaller Ag NPs in DEX-Ag2 compared to larger aggregates in DEX-Ag5

represents higher surface area for the former and therefore, higher surface area readily available to be oxidized and generate Ag^+. Others have also reported that the smaller Ag NPs result in higher resistance to bacterial colonization,[40–44] although direct comparisons are difficult due to differences in times of incubation, assay methods and bacterial strain choice. This is in agreement with RBS studies of the surfaces measured before and after incubation following bacterial test conditions, which indicates that higher content of Ag is leached out of the DEX-Ag2 surface during the bacterial test compared to DEX-Ag5, in particular 26 wt% versus 18 wt%.

To summarize, we have presented a 2-step approach, with the preparation first of colloidal Ag solution in DEX, followed by covalent attachment to the surface. This facile method has great potential for coating medical devices such as plastic catheters and other implantable medical devices. Using simple modifications as previously reported, the colloidal Ag solution in DEX can be grafted to a vast variety of surfaces intended for biomaterials applications, including polymers such as polyurethane[45] and metals, for instance titanium.[46] Further investigations are planned to study whether the inherent biocompatibility of dextran is maintained with the presence of Ag NPs and to test the antimicrobial efficiency of these coatings at longer incubation times (e.g., 48h).

5. Conclusions

A novel approach to prepare a bacterial resistant hybrid biomaterial surface coating is demonstrated. By forming silver nanoparticles *in situ*, the particles become entrapped as the oxidized dextran molecules covalently bind to the surface. These hybrid films show higher efficiency against bacterial colonization when compared to control surfaces. Relative to silicon and bare dextran, these hybrid surfaces are found to strongly inhibit bacterial adhesion.

Acknowledgments

This research was supported by the NIH under Ruth L. Kirschstein National Research Service Award 2T32HL007954 from NIH-NHLBI (M.C.C.F.), R01HL060230 (D.M.E) and NSF DMR08-32802 (R.J.C. and N.J.H.) and NIH HD061053 and DE019901 (N.J.H.). R.J.C. thanks NSF/DMR(DMR09-07493) and NSF/NBIC (DMR05-32802) for facilities use. The authors thank Sangah Gam for performing RBS measurements and Robert C. Ferrier, Jr. for performing TEM images.

References

1. Amir O, Bracey AW, Smart F, Delgado RM, Shah N, Kar B. Texas Heart Institute Journal. 2005; 32:399–401. [PubMed: 16392229]
2. Dowling RD, Gray LA, Etoch SW, Laks H, Marelli D, Samuels L, Entwistle J, Couper G, Vlahakes GJ, Frazier OH. Journal of Thoracic and Cardiovascular Surgery. 2004; 127:131–141. [PubMed: 14752423]
3. Reitsma S, Slaaf DW, Vink H, van Zandvoort M, Egbrink M. Pflugers Archiv-European Journal of Physiology. 2007; 454:345–359. [PubMed: 17256154]
4. Frazier RA, Matthijs G, Davies MC, Roberts CJ, Schacht E, Tendler SJB. Biomaterials. 2000; 21:957–966. [PubMed: 10735473]
5. Martwiset S, Koh AE, Chen W. Langmuir. 2006; 22:8192–8196. [PubMed: 16952261]
6. Piehler J, Brecht A, Hehl K, Gauglitz G. Colloid Surf B-Biointerfaces. 1999; 13:325–336.
7. Ombelli M, Composto RJ, Meng QC, Eckmann DM. Journal of Chromatography B-Analytical Technologies in the Biomedical and Life Sciences. 2005; 826:198–205.
8. Ferrer MCC, Yang S, Eckmann DM, Composto RJ. Langmuir. 2010; 26:14126–14134. [PubMed: 20712352]
9. Massia SP, Stark J, Letbetter DS. Biomaterials. 2000; 21:2253–2261. [PubMed: 11026631]

10. Lok CN, Ho CM, Chen R, He QY, Yu WY, Sun H, Tam PKH, Chiu JF, Che CM. Journal of Biological Inorganic Chemistry. 2007; 12:527–534. [PubMed: 17353996]
11. Berger TJ, Spadaro JA, Bierman R, Chapin SE, Becker RO. Antimicrobial Agents and Chemotherapy. 1976; 10:856–860. [PubMed: 1034467]
12. Feng QL, Wu J, Chen GQ, Cui FZ, Kim TN, Kim JO. J Biomed Mater Res. 2000; 52:662–668. [PubMed: 11033548]
13. Thurman RB, Gerba CP. Crc Critical Reviews in Environmental Control. 1988; 18:295–315.
14. Eby DM, Luckarift HR, Johnson GR. Acs Applied Materials & Interfaces. 2009; 1:1553–1560. [PubMed: 20355960]
15. Roe D, Karandikar B, Bonn-Savage N, Gibbins B, Roullet JB. Journal of Antimicrobial Chemotherapy. 2008; 61:869–876. [PubMed: 18305203]
16. Jain P, Pradeep T. Biotechnology and Bioengineering. 2005; 90:59–63. [PubMed: 15723325]
17. Huang HZ, Yang XR. Carbohydrate Research. 2004; 339:2627–2631. [PubMed: 15476726]
18. Ma YQ, Yi JZ, Zhang LM. Journal of Macromolecular Science Part a-Pure and Applied Chemistry. 2009; 46:643–648.
19. Travan A, Pelillo C, Donati I, Marsich E, Benincasa M, Scarpa T, Semeraro S, Turco G, Gennaro R, Paoletti S. Biomacromolecules. 2009; 10:1429–1435. [PubMed: 19405545]
20. Vigneshwaran N, Nachane RP, Balasubramanya RH, Varadarajan PV. Carbohydrate Research. 2006; 341:2012–2018. [PubMed: 16716274]
21. Vimala K, Sivudu KS, Mohan YM, Sreedhar B, Raju KM. Carbohydrate Polymers. 2009; 75:463–471.
22. Donati I, Travan A, Pelillo C, Scarpa T, Coslovi A, Bonifacio A, Sergo V, Paoletti S. Biomacromolecules. 2009; 10:210–213. [PubMed: 19140690]
23. Ma YQ, Yi JZ, Zhang LM. Journal of Macromolecular Science Part a-Pure and Applied Chemistry. 2009; 46:643–648.
24. Eagye KJ, Nicolau DP, Kuti JL. Seminars in Respiratory and Critical Care Medicine. 2009; 30:116–123. [PubMed: 19199193]
25. Kollef MH, Afessa B, Anzueto A. Jama-Journal of the American Medical Association. 2008; 300:2605–2606.
26. Maki DG, Kluger DM, Crnich CJ. Mayo Clinic Proceedings. 2006; 81:1159–1171. [PubMed: 16970212]
27. Vincent JL, Rello J, Marshall J, Silva E, Anzueto A, Martin CD, Moreno R, Lipman J, Gomersall C, Sakr Y, Reinhart K. Jama-Journal of the American Medical Association. 2009; 302:2323–2329.
28. Warren DK, Quadir WW, Hollenbeak CS, Elward AM, Cox MJ, Fraser VJ. Critical Care Medicine. 2006; 34:2084–2089. [PubMed: 16763511]
29. O'Grady, NP.; Alexander, MA.; Burns, LA.; Dellinger, P.; Garland, J.; Heard, SO.; Lipsett, PA.; Masur, H.; Mermel, LA.; Pearson, ML.; Raad, II.; Randolph, A.; Rupp, ME.; Saint, S. H. I. C. P. A. C (HICPAC). U Health and Human Services. 2011.
30. Stewart PS, Costerton JW. Lancet. 2001; 358:135–138. [PubMed: 11463434]
31. Berra L, De Marchi L, Yu ZX, Laquerriere P, Baccarelli A, Kolobow T. Anesthesiology. 2004; 100:1446–1456. [PubMed: 15166564]
32. Rello J, Kollef M, Diaz E, Sandiumenge A, del Castillo Y, Corbella X, Zachskorn R. Critical Care Medicine. 2006; 34:2766–2772. [PubMed: 16957639]
33. Zhao H, Heindel ND. Pharmaceutical Research. 1991; 8:400–402. [PubMed: 1711201]
34. Lee HS, Eckmann DM, Lee D, Hickok NJ, Composto RJ. Langmuir. 2011; 27:12458–12465. [PubMed: 21894981]
35. Vinod VTP, Sashidhar RB, Suresh KI, Rao BR, Saradhi UVRV, Rao TP. Food Hydrocolloids. 2008; 22:899–915.
36. Willets KA, Van Duyne RP. Annual Review of Physical Chemistry. 2007; 58:267–297.
37. Ombelli, M.; Eckmann, DM.; Composto, RJ. Biomimetic dextran coatings on silicon wafers : thin film properties and wetting. Boston: 2002.
38. Rinaudo M. Polym Int. 2008; 57:397–430.

39. Singh M, Sinha I, Mandal RK. Materials Letters. 2009; 63:425–427.
40. Amato E, Diaz-Fernandez YA, Taglietti A, Pallavicini P, Pasotti L, Cucca L, Milanese C, Grisoli P, Dacarro C, Fernandez-Hechavarria JM, Necchi V. Langmuir. 2011; 27:9165–9173. [PubMed: 21736306]
41. D'Britto V, Kapse H, Babrekar H, Prabhune AA, Bhoraskar SV, Premnath V, Prasad BLV. Nanoscale. 2011; 3:2957–2963. [PubMed: 21643585]
42. Lischer S, Korner E, Balazs DJ, Shen D, Wick P, Grieder K, Haas D, Heuberger M, Hegemann D. Journal of the Royal Society Interface. 2011; 8:1019–1030.
43. Shameli K, Bin Ahmad M, Zargar M, Yunus W, Rustaiyan A, Ibrahim NA. International Journal of Nanomedicine. 2011; 6:581–590. [PubMed: 21674015]
44. Zhao LZ, Wang HR, Huo KF, Cui LY, Zhang WR, Ni HW, Zhang YM, Wu ZF, Chu PK. Biomaterials. 2011; 32:5706–5716. [PubMed: 21565401]
45. Tsai IY, Tomczyk N, Eckmann JI, Composto RJ, Eckmann DM. Colloid Surf B-Biointerfaces. 2011; 84:241–252.
46. Shi Z, Neoh KG, Kang ET, Poh C, Wang W. Tissue Engineering Part A. 2009; 15:417–426. [PubMed: 18837650]

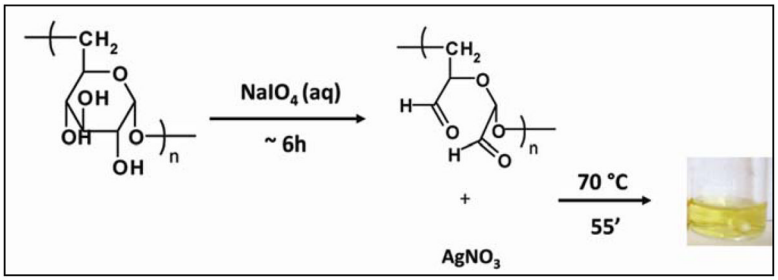

Figure 1.

In situ formation of Ag NPs in dextran (DEX) solution. DEX is first oxidized with sodium metaperiodate. This reaction leads to formation of two aldehydes per anhydroglucose oxidized unit. DEX solution is then used to reduce silver nitrate to silver.

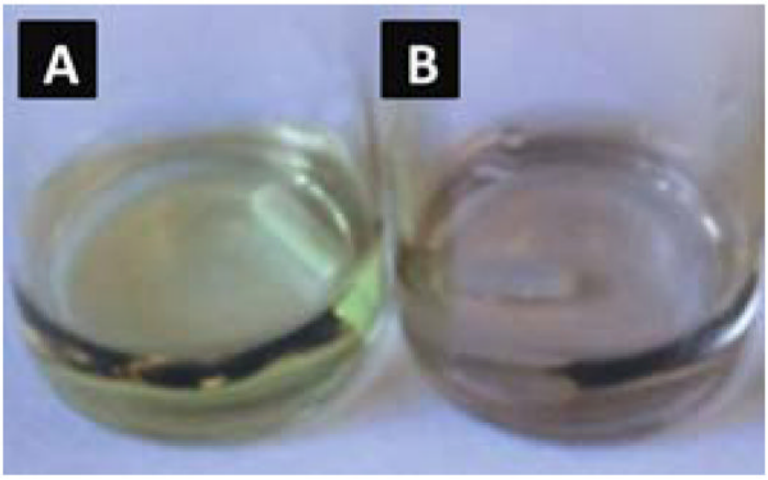

Figure 2.
Colloidal silver in DEX-Ag5 (a) as prepared and (b) after 1 h as aggregation occurs.

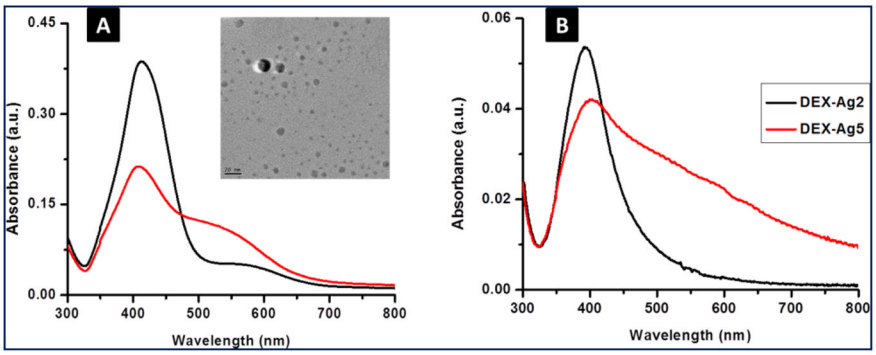

Figure 3.

UV-VIS spectroscopy for silver embedded in dextran (DEX-Ag) (a) in solution ($\lambda = 412 \pm 2$ nm) and (b) grafted on to the surface ($\lambda = 400 \pm 5$nm) for 2 mM and 5 mM silver nitrate concentrations, DEX-Ag2 and DEX-Ag5, respectively. The peaks correspond to the surface plasmon resonance of silver. DEX-Ag2 shows mainly a sharp peak indicating narrow particle size distribution, whereas a broader band characterizes DEX-Ag5. A slight shift to the blue results from attaching DEX containing Ag NPs onto the surface compared to solution. TEM micrograph of silver nanoparticles embedded in DEX-Ag2 showing spherical particles (scale bar, 20 nm). The average diameter of the silver nanoparticles is 4.8 ± 2.6 nm.

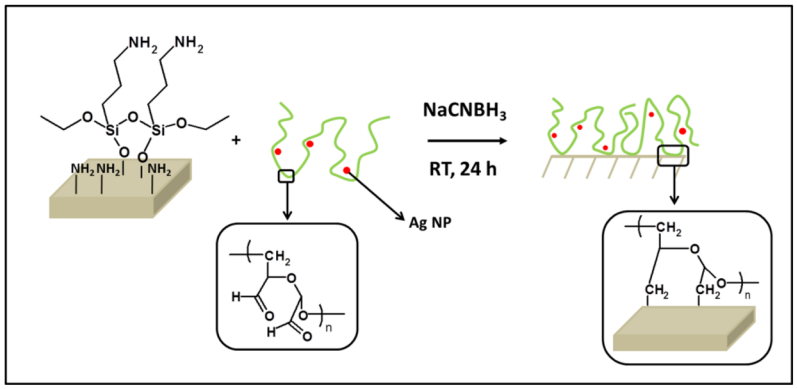

Figure 4.

The grafting process: Previously aminated surfaces are immersed into a DEX solution containing Ag NPs (DEX-Ag solution). The aldehydes present in DEX react with the amines to form imines, which are further reduced to amines with sodium cyanoborohydride. As the reaction proceeds, the Ag NPs are entrapped in the DEX network, which is covalently attached to the surface.

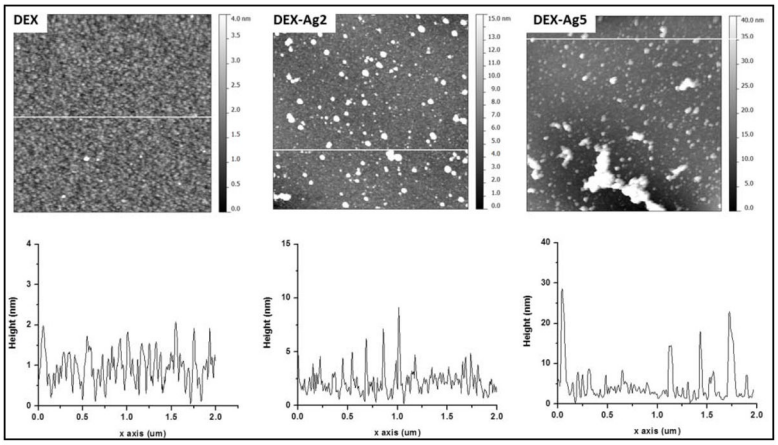

Figure 5.

Top: AFM topography images of grafted DEX (DEX) and grafted DEX with trapped silver nanoparticles prepared using silver nitrate concentrations of 2 mM (DEX-Ag2) and 5 mM (DEX-Ag5). The scan size is 2 x 2 μm^2. The grafted dextran surface shows a uniform distribution of ~ 50 nm features and 2 nm height across a relatively smooth surface. The surfaces with grafted dextran containing Ag NPs show both individual Ag NPs (~ 5 nm) as well as larger cluster uniformly distributed across the film. Larger and irregularly shaped aggregates are observed in DEX-Ag5. Note the differences in z scale within the images, z = 4nm for DEX, z = 15 nm for DEX-Ag2 and z = 40 nm for DEX-Ag. Bottom: line scan across white line of the corresponding upper topography image.

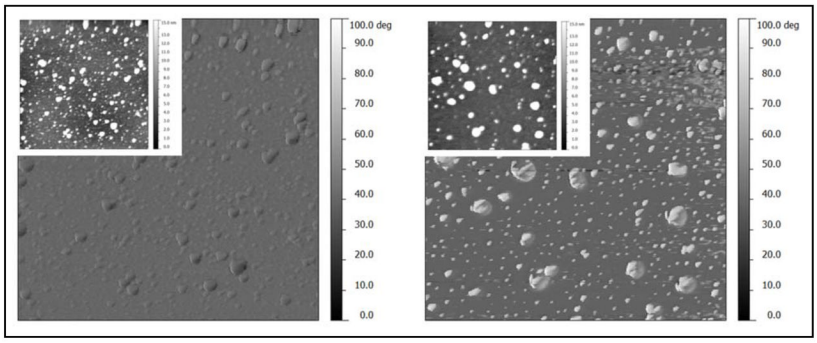

Figure 6.

AFM phase images of DEX with embedded silver nanoparticles prepared using 2 mM silver nitrate concentration (DEX-Ag2) as prepared (left) and after UVO exposure for 15 min (right) and corresponding topography images (insets). The scan size is 2 x 2 μm^2. The DEX-Ag2 surface shows individual Ag NPs and larger clusters uniformly distributed across the film. Exposure to UVO leads to an increase in the number of individual Ag NPs and clusters (right), confirming the presence of Ag NPs embedded in the film.

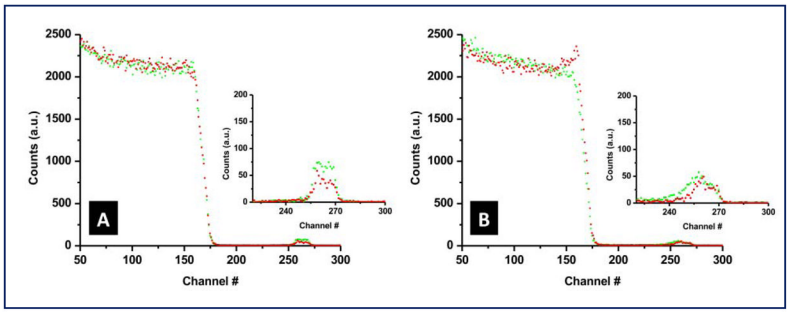

Figure 7.

Rutherford backscattering spectrometry (RBS) for DEX with trapped Ag NPs for (a) DEX-Ag2 and (b) DEX-Ag5 films before (green) and after (red) exposure to conditions that mimic bacterial testing. The insets magnify the region corresponding to the silver peaks. The amount of silver (i.e., area under the curve) that leaches out of the surfaces is 26% for DEX-Ag2 and 18% for DEX-Ag5.

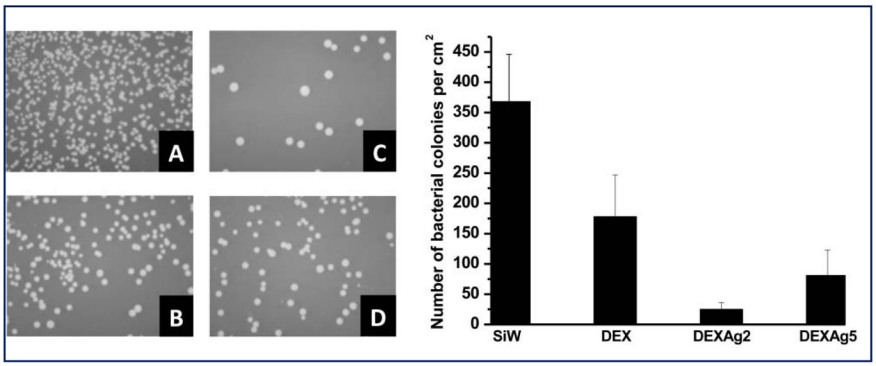

Figure 8.

Left: Optical images of (a) silicon (SiW), (b) DEX and (c) DEX-Ag2 and (d) DEX-Ag5 after inoculation with bacteria for 6 h. The images correspond to a sample size of 1 x 1.25 cm^2. Right: comparison of the number of bacterial colonies per cm^2 for each surface studied. The presence of Ag NPs (c and d) significantly enhances surface resistance to bacterial colonization compared to SiW (a) and DEX (b). DEX-Ag2 shows the greatest resistance to bacteria colonization.